SUPPORTING INFORMATION

Gas Phase Assembling of Dirhodium Units into a Novel Organometallic Ladder: Structural and DFT Study

*Alexander S. Filatov, Andrey Yu. Rogachev, Marina A. Petrukhina**

Department of Chemistry, University at Albany, SUNY, Albany, New York 12222

DFT Analysis

Orbital Interaction Analysis. DFT/B3LYP method was used to calculate the orbital model of metal-metal bonding and anti-bonding interactions for dirhodium(II,II) tetratrifluoroacetate. These orbitals, designated as σ, π, δ, δ^*, π^*, and σ^*, define the bonding and the reactivity of the dirhodium units. The energetic ordering of the Rh–Rh bonding and anti-bonding orbitals in dirhodium(II,II) tetratrifluoroacetate is still not well substantiated. From the photoelectron spectroscopy point of view, it can only be concluded that the δ^* and π^* ionization energies are similar within the spread of vibrational energies with excitation (0.2 eV). Calculations using different levels of theory provided different energetic ordering of these two orbitals.[1] Herein we performed calculations using higher level of theory than that reported previously (hybrid functional over non-hybrid functional). This supported a ground-state configuration of $\sigma^2\pi^4\delta^2\pi^{*4}\delta^{*2}$ for the $Rh_2(O_2CCF_3)_4$ molecule. The difference between δ^* and π^* orbitals is very small (0.0077 hartrees, 0.21 eV) and can be considered as negligible. Therefore, these orbitals are nearly degenerate (Scheme 1).

Scheme 1. Molecular orbital diagram for the unligated $Rh_2(O_2CCF_3)_4$ complex (DFT/B3LYP/LANL2DZ/6-311G(d,p)).

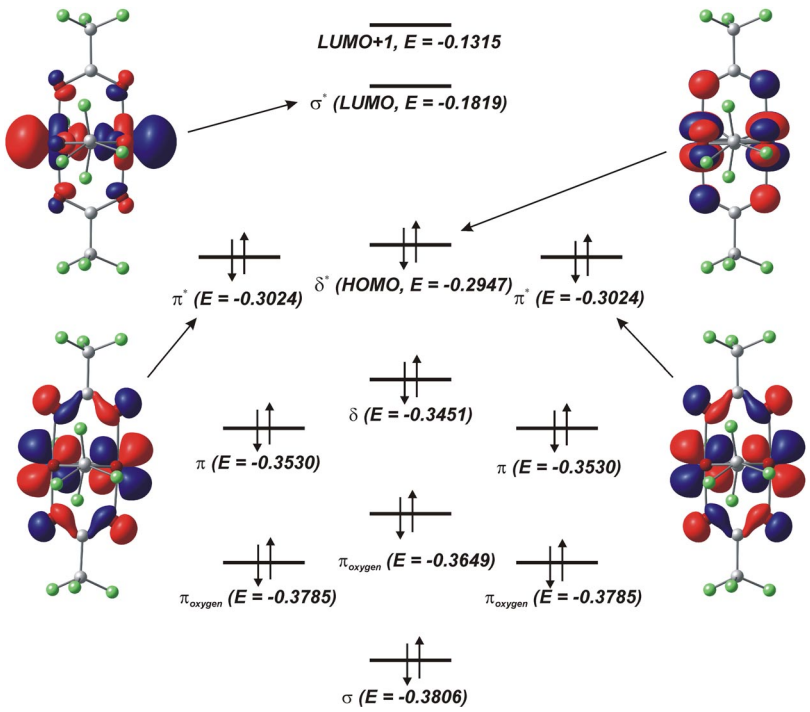

Some important features of this electronic system should be pointed out. First, the lowest unoccupied molecular orbital (LUMO) lies 0.0504 hartrees (1.37 eV) lower than the next unoccupied molecular orbital (LUMO+1). Since this difference in energy precludes the possibility to donate electrons into the LUMO+1, only the LUMO can be considered as an acceptor of electrons from the donor aromatic system. Second, the energy degeneration of the two π^* orbitals and the δ^* orbital could make all these three orbitals usable for π back-donation. However, the requirement for the accepting orbital to be the σ^*, which is the d_z^2 orbital, causes a back-donating orbital to include a *z* component. This excludes the δ^* orbital, which is the d_{xy} orbital, from our future considerations. This leaves the σ^* orbital as an acceptor of electrons and

one of the π^* orbitals as a donor of electrons in respect to the ligand. Calculated geometry and selected geometry parameters for the $Rh_2(O_2CCF_3)_4$ molecule are presented in Figure 1 and Table 1.

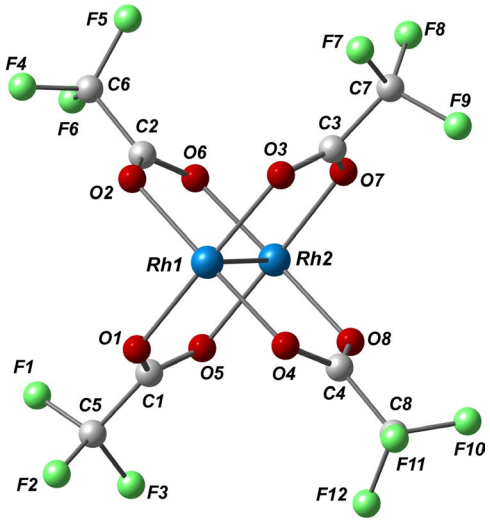

Figure 1. Equilibrium geometry configuration of $Rh_2(O_2CCF_3)_4$ (DFT/B3LYP/LANL2DZ/3-21G(d)).

Table 1. Equilibrium geometry parameters for $Rh_2(O_2CCF_3)_4$ (DFT/B3LYP/LANL2DZ/3-21G(d), given for symmetry unique atoms).

Bond	d, Å	Angle	ω, °
Rh(1) – Rh(2)	2.41	∠Rh(1) – Rh(2) – O(5)	88.5
Rh(1) – O(1)	2.05	∠Rh(2) – Rh(1) – O(1)	88.5
Rh(2) – O(5)	2.05	∠Rh(1) – O(1) – C(1)	118.2
O(1) – C(1)	1.28	∠Rh(2) – O(5) – C(1)	118.1
O(5) – C(1)	1.28	∠O(1) – C(1) – O(5)	126.8
C(1) – C(5)	1.53	∠O(1) – C(1) – C(5)	117.1

C(5) – F(1)	1.36	∠O(5) – C(1) – C(5)	116.0
C(5) – F(2)	1.36		
C(5) – F(3)	1.36		

DFT calculations results for the ligand, $C_{24}H_{26}$, showed that the optimized geometry configuration corresponds to one having all benzene rings lying in parallel planes (Figure 2).

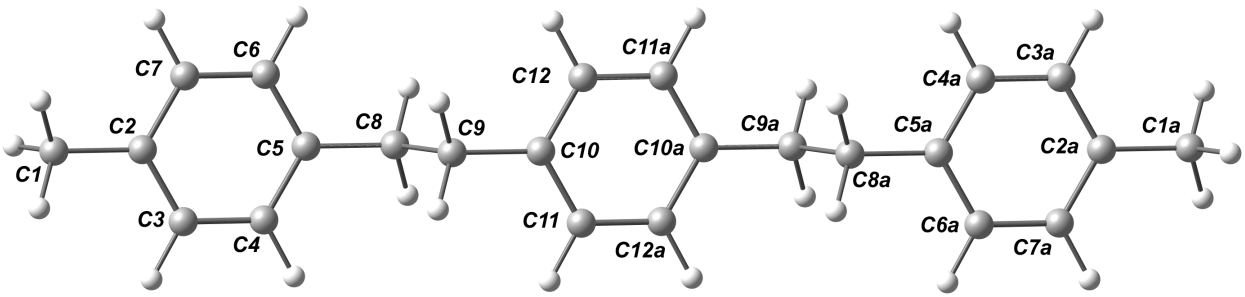

Figure 2. The equilibrium geometry configuration of **1**, $C_{24}H_{26}$ (DFT/B3LYP/3-21G(d)).

These results (Table 2) are in a good accord with the experimental X-ray data.

Table 2. Equilibrium geometry parameters for **1** (DFT/B3LYP/3-21G(d), given for symmetry unique atoms).

Bond	d, Å	Angle	ω, º
C(1) – C(2)	1.52	∠C(1) – C(2) – C(3)	120.9
C(2) – C(3)	1.40	∠C(2) – C(3) – C(4)	120.9
C(3) – C(4)	1.39	∠C(3) – C(4) – C(5)	120.9
C(4) – C(5)	1.40	∠C(4) – C(5) – C(8)	120.9
C(5) – C(8)	1.52	∠C(5) – C(8) – C(9)	111.4

C(8) – C(9)	1.56	∠C(3) – C(2) – C(7)	118.2
C(9) – C(10)	1.52	∠C(4) – C(5) – C(6)	118.2
C(10) – C(11)	1.40	∠C(8) – C(9) – C(10)	111.3
C(11) – C(12a)	1.39	∠C(9) – C(10) – C(12)	120.9
		∠C(10) – C(12) – C(11a)	120.9
		∠C(11) – C(10) – C(12)	118.2

Analysis of the electronic structure of the ligand shows that all six highest occupied molecular orbitals are suitable to interact with the LUMO of dirhodium tetratrifluoroacetate by the symmetry considerations (Scheme 2).

Scheme 2. Molecular orbital diagram for **1** (DFT/B3LYP/6-311G(d,p)).

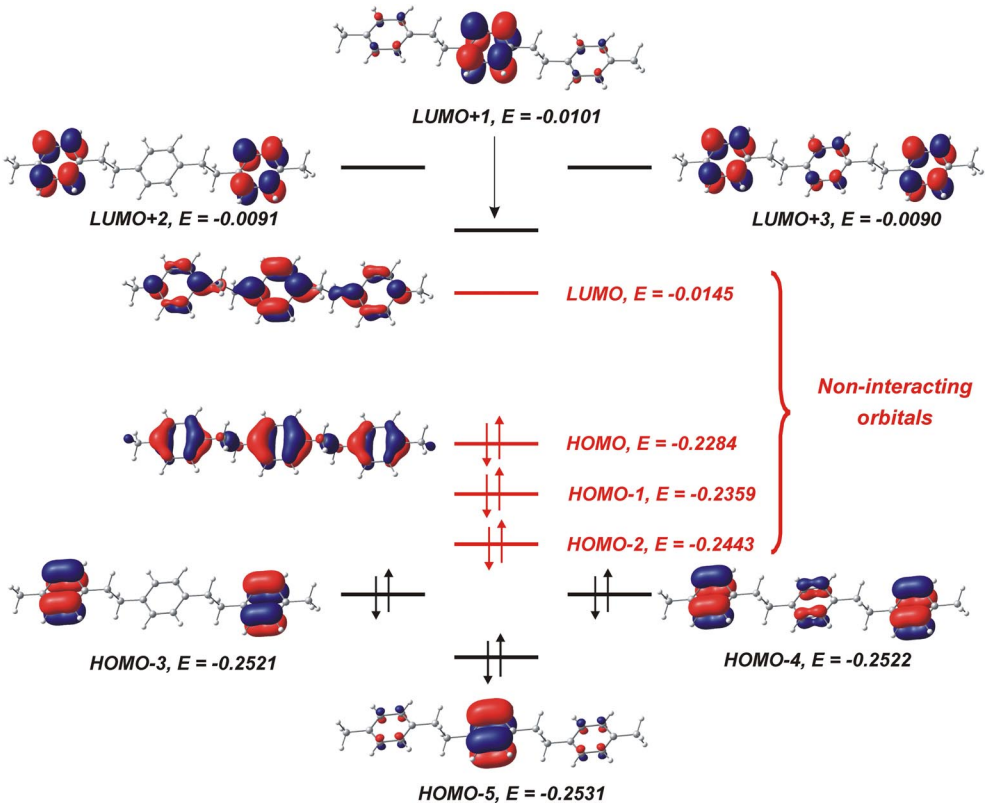

But what is more important in this case is a possibility to have the metal-ligand back-donation in addition to the ligand-metal donation. So we may exclude unsuitable molecular orbitals using the back-donation condition as a required prerequisite. Thus, the only suitable pairs of orbitals for interaction are HOMO-3/LUMO+2 and HOMO-4/LUMO+3. Now we can construct the orbital interaction diagram for organometallic complex. It is interesting to note that the bonding interaction in this case is not a simple $2e^-$ - 2 orbital interaction of the filled and empty orbitals but, in fact, more complicated $4e^-$ - 3 orbital interaction. Similar interactions with some other dimetal units have been mentioned previously.[2] Back-donation bonding provides a small destabilizing energetic effect (*ca*. 0.44 eV) on the final structure of the $[Rh_2(O_2CCF_3)_4 \cdot (C_{24}H_{26})]$ complex (Scheme 3).

Scheme 3. Orbital interaction diagram for the $[Rh_2(O_2CCF_3)_4 \cdot (C_{24}H_{26})]$ complex.

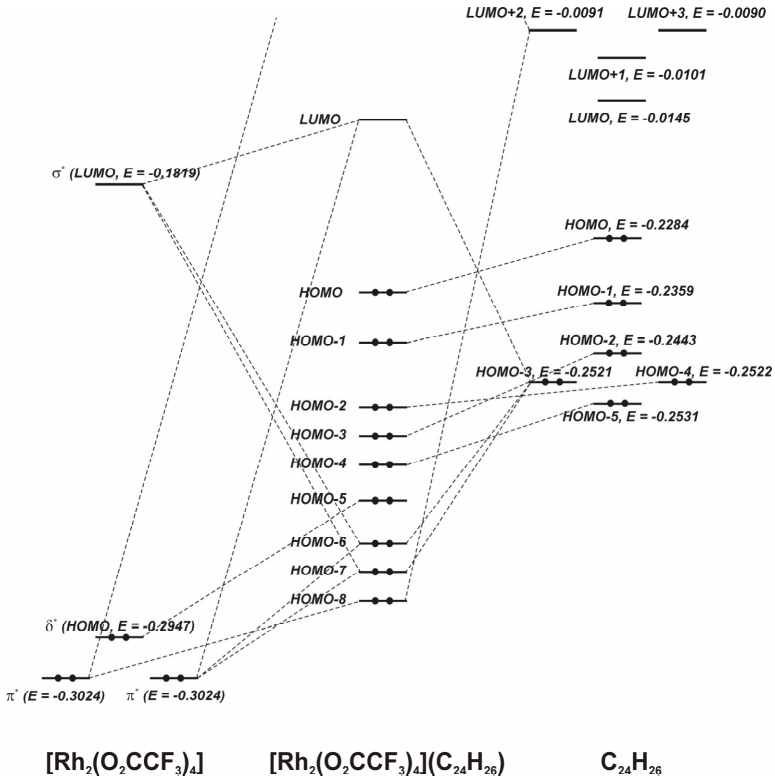

Calculated geometry and selected geometry parameters for the $[Rh_2(O_2CCF_3)_4 \cdot (C_{24}H_{26})]$ complex are presented in Figure 3 and Table 3.

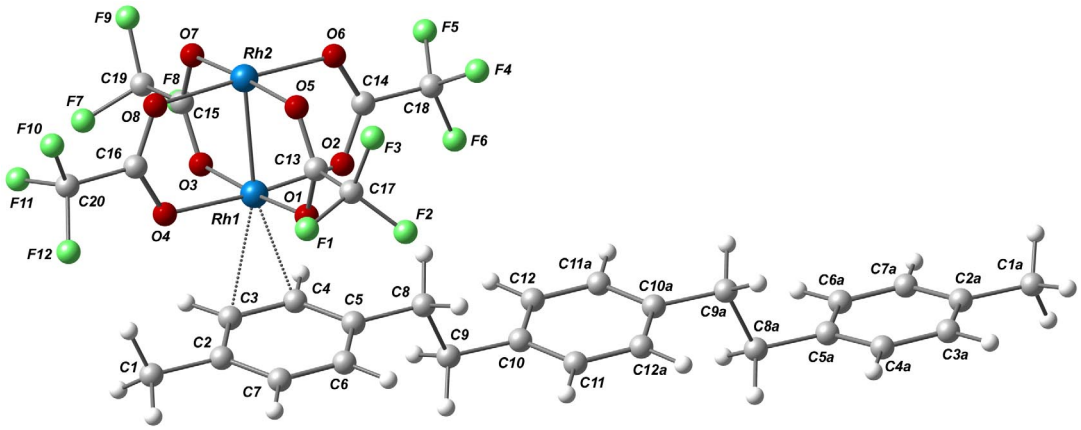

Figure 3. The equilibrium geometry configuration of the $[Rh_2(O_2CCF_3)_4 \cdot (C_{24}H_{26})]$ complex (DFT/B3LYP/LANL2DZ/3-21G(d)).

Table 3. Equilibrium geometry parameters for the $[Rh_2(O_2CCF_3)_4 \cdot (C_{24}H_{26})]$ complex (DFT/B3LYP/LANL2DZ/3-21G(d)).

Bond	d, Å	Angle	ω, °
Rh(1) – Rh(2)	2.44	∠Rh(1) – Rh(2) – O(5)	88.7
Rh(1) – O(1)	2.05	∠Rh(1) – Rh(2) – O(6)	88.6
Rh(1) – O(2)	2.06	∠Rh(1) – Rh(2) – O(7)	88.8
Rh(1) – O(3)	2.05	∠Rh(1) – Rh(2) – O(8)	88.7
Rh(1) – O(4)	2.05	∠Rh(2) – Rh(1) – O(1)	87.3
Rh(2) – O(5)	2.05	∠Rh(2) – Rh(1) – O(2)	87.3
Rh(2) – O(6)	2.05	∠Rh(2) – Rh(1) – O(3)	88.2

Rh(2) – O(7)	2.06	∠Rh(2) – Rh(1) – O(4)	87.2
Rh(2) – O(8)	2.06	∠Rh(1) – O(1) – C(13)	119.0
Rh(1) – C(3)	2.62	∠Rh(1) – O(2) – C(14)	119.0
Rh(1) – C(4)	2.59	∠Rh(1) – O(3) – C(15)	118.0
C(13) – O(1)	1.29	∠Rh(1) – O(4) – C(16)	119.1
C(13) – O(5)	1.28	∠Rh(2) – O(5) – C(13)	118.5
C(14) – O(2)	1.28	∠Rh(2) – O(6) – C(14)	117.7
C(14) – O(6)	1.28	∠Rh(2) – O(7) – C(15)	118.6
C(15) – O(3)	1.29	∠Rh(2) – O(8) – C(16)	117.6
C(15) – O(7)	1.28	∠O(1) – C(13) – O(5)	127.5
C(16) – O(4)	1.28	∠O(2) – C(14) – O(6)	127.3
C(16) – O(8)	1.28	∠O(3) – C(15) – O(7)	127.4
C(13) – C(17)	1.53	∠O(4) – C(16) – O(8)	127.4
C(14) – C(18)	1.53	∠O(1) – C(13) – C(17)	114.9
C(15) – C(19)	1.53	∠O(2) – C(14) – C(18)	116.2
C(16) – C(20)	1.53	∠O(3) – C(15) – C(19)	114.7
C(17) – F(1)	1.37	∠O(4) – C(16) – C(20)	114.9
C(17) – F(2)	1.37	∠O(5) – C(13) – (17)	117.6
C(17) – F(3)	1.37	∠O(6) – C(14) – C(18)	116.4
C(18) – F(4)	1.37	∠O(7) – C(15) – C(19)	117.8
C(18) – F(5)	1.37	∠O(8) – C(16) – C(20)	117.6
C(18) – F(6)	1.37	∠C(3) – Rh(1) – C(4)	31.6
C(19) – F(7)	1.37	∠Rh(1) – C(3) – C(4)	73.1
C(19) – F(8)	1.37	∠Rh(1) – C(4) – C(3)	75.4
C(19) – F(9)	1.37	∠C(1) – C(2) – C(3)	120.4
C(20) – F(10)	1.37	∠C(1) – C(2) – C(7)	121.8
C(20) – F(11)	1.37	∠C(2) – C(3) – C(4)	120.7
C(20) – F(12)	1.37	∠C(3) – C(4) – C(5)	120.8
C(1) – C(2)	1.52	∠C(4) – C(5) – C(8)	120.9

C(2) – C(3)	1.41	∠C(4) – C(5) – C(6)	117.8
C(2) – C(7)	1.39	∠C(5) – C(6) – C(7)	120.9
C(3) – C(4)	1.41	∠C(6) – C(5) – C(8)	121.3
C(4) – C(5)	1.41	∠C(6) – C(7) – C(2)	121.4
C(5) – C(6)	1.39	∠C(7) – C(2) – C(3)	117.8
C(5) – C(8)	1.52	∠C(5) – C(8) – C(9)	111.8
C(6) – C(7)	1.40	∠C(8) – C(9) – C(10)	111.2
C(8) – C(9)	1.56	∠C(9) – C(10) – C(11)	120.4
C(9) – C(10)	1.52	∠C(9) – C(10) – C(11a)	121.2
C(10) – C(11)	1.40	∠C(10) – C(11) – C(12a)	120.9
C(11) – C(12a)	1.39	∠C(11) – C(12a) – C(10a)	120.8
C(12a) – C(10a)	1.40	∠C(12) – C(10a) – C(9a)	120.7
C(10a) – C(12)	1.40	∠C(12a) – C(10a) – C(12)	118.3
C(12) – C(11a)	1.40	∠C(10a) – C(12) – C(11a)	120.9
C(11a) – C(10)	1.40	∠C(12) – C(11a) – C(10)	120.8
C(10a) – C(9a)	1.52	∠C(11a) – C(10) – C(11)	118.3
C(9a) – C(8a)	1.56	∠C(10a) – C(9a) – C(8a)	111.4
C(8a) – C(5a)	1.52	∠C(9a) – C(8a) – C(5a)	111.4
C(5a) – C(4a)	1.40	∠C(8a) – C(5a) – C(4a)	120.9
C(4a) – C(3a)	1.40	∠C(8a) – C(5a) – C(6a)	120.9
C(3a) – C(2a)	1.40	∠C(5a) – C(4a) – C(3a)	120.9
C(2a) – C(7a)	1.40	∠C(4a) – C(3a) – C(2a)	120.9
C(7a) – C(6a)	1.39	∠C(3a) – C(2a) – C(1a)	121.2
C(6a) – C(5a)	1.40	∠C(3a) – C(2a) – C(7a)	118.2
C(2a) – C(1a)	1.52	∠C(2a) – C(7a) – C(6a)	120.9
		∠C(7a) – C(6a) – C(5a)	120.9
		∠C(6a) – C(5a) – C(4a)	118.2
		∠C(1a) – C(2a) – C(7a)	120.5

After coordination of the first dirhodium unit to the aromatic ligand, the electronic structure is highly perturbed in such a way that the following coordination of the second dirhodium unit is only possible to the C3a–C4a or C6a–C7a bonds. The requirement to find suitable orbitals for the metal-ligand back-donation before choosing the occupied molecular orbitals that may further interact with the second dirhodium unit should be stressed out here again (Figure 4).

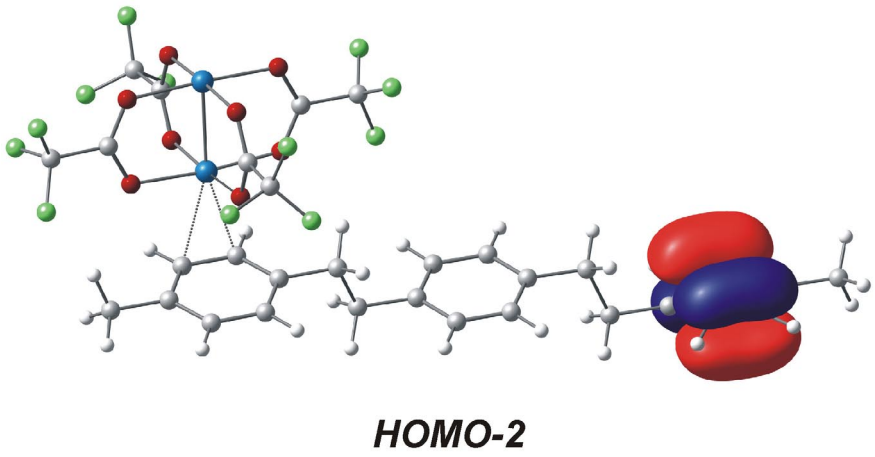

Figure 4. Donor orbital of the $Rh_2(O_2CCF_3)_4 \cdot C_{24}H_{26}$ complex (DFT/B3LYP/LANL2DZ/6-311G(d,p)).

Taking into account bond orders for these bonds, the C6a–C7a bond seems a more preferable attacking site for the next dirhodium unit over the C3a–C4a bond (Table 4, see Tables 5-6 for comparison).

Table 4. Bond orders in the $[Rh_2(O_2CCF_3)_4 \cdot (C_{24}H_{26})]$ complex (DFT/B3LYP/LANL2DZ/6-311G(d,p)).

Bond	Bond order	Bond	Bond order

C(1) – C(2)	1.031	C(5a) – C(6a)	1.395
C(2) – C(3)	1.333	C(6a) – C(7a)	1.446
C(3) – C(4)	1.381	C(7a) – C(2a)	1.395
C(4) – C(5)	1.332	C(2a) – C(3a)	1.405
C(5) – C(6)	1.448	C(3a) – C(4a)	1.435
C(6) – C(7)	1.378	C(4a) – C(5a)	1.403
C(1) – C(7)	1.448	C(1a) – C(2a)	1.028
C(5) – C(8)	1.013	Rh(1) – Rh(2)	0.665
C(8) – C(9)	0.982	Rh(1) – O(1)	0.350
C(9) – C(10)	1.012	Rh(1) – O(2)	0.341
C(10) – C(11)	1.394	Rh(1) – O(3)	0.346
C(11) – C(12a)	1.446	Rh(1) – O(4)	0.343
C(10) – C(12)	1.404	Rh(2) – O(5)	0.338
C(12a) – C(10a)	1.394	Rh(2) – O(6)	0.337
C(11a) – C(12)	1.404	Rh(2) – O(7)	0.330
C(11a) – C(10a)	1.404	Rh(2) – O(8)	0.333
C(10a) – C(9a)	1.013	Rh(1) – C(3)	0.051
C(9a) – C(8a)	0.984	Rh(1) – C(4)	0.049
C(8a) – C(5a)	1.012		

Table 5. Bond orders in **1**, $C_{24}H_{26}$ (DFT/B3LYP/6-311G(d,p), given for symmetry unique atoms).

Bond	Bond order	Bond	Bond order
C(1) – C(2)	1.028	C(8) – C(9)	0.983
C(2) – C(3)	1.400	C(9) – C(10)	1.013
C(3) – C(4)	1.441	C(10) – C(11)	1.399
C(4) – C(5)	1.400	C(11) – C(12a)	1.440
C(5) – C(8)	1.021		

Table 6. Bond orders in $Rh_2(O_2CCF_3)_4$ (DFT/B3LYP/LANL2DZ/6-311G(d,p)).

Bond	Bond order	Bond	Bond order
Rh(1) – Rh(2)	0.791	O(1) – C(1)	1.403
Rh(1) – O(1)	0.351	O(5) – C(1)	1.403
Rh(1) – O(5)	0.351	C(1) – C(5)	0.911

The Rh–Rh bond order in the dirhodium complex is substantially decreased upon coordination of the arene ligand due to additional electrons in anti-bonding orbitals of the dimetal unit donated by the ligand. This is in a good agreement with the X-ray data that showed elongation of the Rh–Rh bond in **2** compare to that in the unligated $Rh_2(O_2CCF_3)_4$ complex. The bond orders for the C(3)–C(4) and C(6)–C(7) bonds are also decreased due to back-donation of electrons from the metal-metal bond into anti-bonding orbitals of the ligand. The C–C bond orders in uncoordinated benzene rings in the $[Rh_2(O_2CCF_3)_4 \cdot (C_{24}H_{26})]$ complex remain approximately the same as in free ligand. Small but considerable bond order was found for the Rh–C bond in organometallic complex (Table 4). This is consistent with the charge distributions for the molecules (Tables 7-9).

Table 7. Charge distribution in **1** (DFT/B3LYP/6-311G(d,p), given for symmetry unique atoms).

Atom	Charge	Atom	Charge
C(1)	-0.585	C(8)	-0.379
C(2)	-0.019	C(9)	-0.379
C(3)	-0.199	C(10)	-0.022

C(4)	-0.199	C(12)	-0.199
C(5)	-0.024		

Table 8. Charge distribution in $Rh_2(O_2CCF_3)_4$ (DFT/B3LYP/LANL2DZ/6-311G(d,p), given for symmetry unique atoms).

Atom	Charge	Atom	Charge
Rh(1)	+0.975	C(5)	+1.041
Rh(2)	+0.975	F(1)	-0.345
O(1)	-0.626	F(2)	-0.345
O(5)	-0.626	F(3)	-0.345
C(1)	+0.750		

Table 9. Charge distribution in the $[Rh_2(O_2CCF_3)_4 \cdot (C_{24}H_{26})]$ complex (DFT/B3LYP/LANL2DZ/6-311G(d,p)).

Atom	Charge	Atom	Charge
Rh(1)	+0.966	C(1)	-0.594
Rh(2)	+0.902	C(2)	-0.006
O(1)	-0.624	C(3)	-0.231
O(2)	-0.628	C(4)	-0.236
O(3)	-0.636	C(5)	-0.011
O(4)	-0.631	C(6)	-0.169
O(5)	-0.624	C(7)	-0.175
O(6)	-0.628	C(8)	-0.392
O(7)	-0.624	C(9)	-0.378
O(8)	-0.624	C(10)	-0.024
C(13)	+0.746	C(11)	-0.199

C(14)	+0.749	C(12)	-0.196
C(15)	+0.749	C(1a)	-0.598
C(16)	+0.748	C(2a)	-0.019
C(17)	+1.041	C(3a)	-0.199
C(18)	+1.042	C(4a)	-0.199
C(19)	+1.041	C(5a)	-0.025
C(20)	+1.042	C(6a)	-0.198
F(1)	-0.349	C(7a)	-0.198
F(2)	-0.346	C(8a)	-0.378
F(3)	-0.340	C(9a)	-0.379
F(4)	-0.343	C(10a)	-0.020
F(5)	-0.347	C(11a)	-0.197
F(6)	-0.343	C(12a)	-0.198
F(7)	-0.347		
F(8)	-0.339		
F(9)	-0.347		
F(10)	-0.338		
F(11)	-0.352		
F(12)	-0.346		

It is worth mentioning that the rhodium atoms in the dirhodium unit acquire different amount of negative charge: when the charge on the rhodium atom involved in coordination remained unchanged, the charge on the uncoordinated rhodium atom is greatly decreased. That confirms that “unused” rhodium atom can work as an electron sink adopting some additional electrons from the ligand (Table 9).

Flexibility of a Molecular Skeleton in $C_{24}H_{26}$. In the structure of **2** the central ring of the ligand was rotated at *ca*. 26° upon coordination of dirhodium units. To probe a rotation freedom

of a molecular skeleton of the organic ligand, the potential energy curve was modeled at *ab initio* Hartree-Fock level with the 6-31G(d,p) basis set. The rotational barrier of the central ring was calculated to be *ca*. 6.4 kcal/mol. It is almost 6 times higher than that in the parent dehydrogenated compound.[3] To check if the rotation of this benzene ring was mostly caused by the steric repulsions between the trifluoroacetate groups and the central benzene ring, DFT geometry optimization was carried out with the $\{[Rh_2(O_2CH)_4]_2 \cdot C_{24}H_{26}\}$ complex. Geometry truncation of trifluoromethyl groups removed steric interactions and allowed the middle ring to be freely rotated. As a result of this optimization all benzene rings were found to lie in parallel planes as there were in the free ligand. This clearly shows predominant steric reasons for the rotation of the middle ring of the aromatic ligand in the structure of **2** (Figure 8).

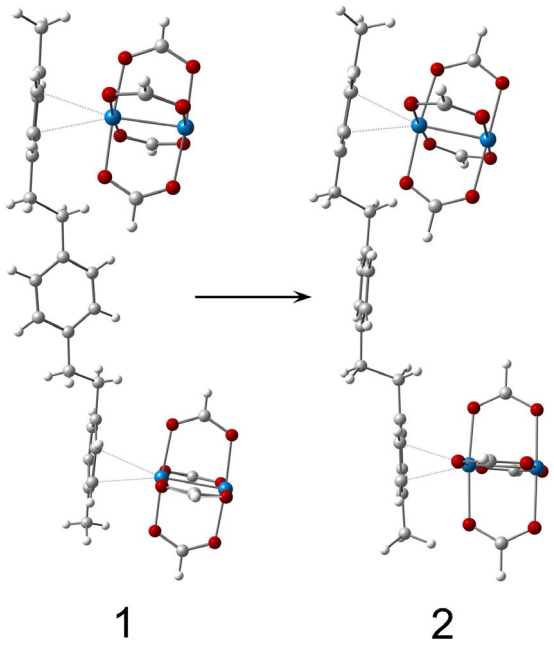

Figure 5. Starting (1) and ending (2) geometry configurations for the geometry optimization of the $\{[Rh_2(O_2CH)_4]_2 \cdot C_{24}H_{26}\}$ complex (DFT/B3LYP/LANL2DZ/3-21G(d)).

To estimate the thermodynamic stability of the $[Rh_2(O_2CCF_3)_4 \cdot C_{24}H_{26}]$ complex, the bonding energy was calculated to be 11.13 kcal/mol using the following formula:

$E[bonding] = E[Rh_2(O_2CCF_3)_4 \cdot C_{24}H_{26}] - E[C_{24}H_{26}] - E[Rh_2(O_2CCF_3)_4]$.

References

(1) Lichtenberger, D. L.; Pollard, J. R.; Lynn, M. A.; Cotton, F.A.; Feng, X. *J. Am. Chem. Soc*., **2000**, *122*, 3182-3190.

(2) Bursten, B. E.; Chisholm, M. H.; D'Acchioli, J. S. *Inorg. Chem.* **2005**, *44*, 5571-5579.

(3) Filatov, A. S.; Petrukhina, M. A. *Acta Cryst*. **2005**, *c61*, o193-o194.